

Non-minimally Coupled Running Curvaton: A Unified Approach to Early-Universe Inflation and Phantom Dark Energy

Bichu Li* and Lei-Hua Liu†

Department of Physics, College of Physics, Mechanical and Electrical Engineering, Jishou University, Jishou 416000, China

(Dated: February 13, 2026)

Recent observations from the Dark Energy Spectroscopic Instrument (DESI) 2025, combined with CMB and SNIa data, indicate a preference for a dynamical dark energy equation of state that crosses the phantom divide ($w < -1$). This finding challenges the standard Λ CDM model and minimally coupled scalar field scenarios, including the original Running Curvaton model, which is typically constrained to the quintessence regime. In this work, we propose a unified cosmological framework by extending the Running Curvaton model via a non-minimal gravitational coupling of the form $\xi\chi^2R$. We demonstrate that this geometric modification allows the effective equation of state to naturally evolve from a quintessence-like to a phantom-like regime in the Jordan frame, thereby providing a superior fit to the DESI observational contours ($w_0 > -1, w_a < 0$). Crucially, we show that the introduction of non-minimal coupling does not compromise the model's success in describing the early universe. Through a parameter re-tuning mechanism involving the coupling constant ($g_0^{obs} = g_0 + 2\xi$), the predictions for the primordial power spectrum (spectral index n_s) and local-type non-Gaussianity (f_{NL}) remain strictly preserved and consistent with Planck data. Furthermore, we perform a comprehensive stability analysis within the Horndeski framework, verifying that the model remains free from ghost and gradient instabilities ($c_s^2 = 1$). Our results suggest that the non-minimally coupled Running Curvaton offers a robust, stable, and unified description of inflation and late-time accelerated expansion compatible with the latest precision cosmology data.

I. INTRODUCTION

The standard cosmological model, Λ CDM, has been remarkably successful in explaining a wide range of observations, from the Cosmic Microwave Background (CMB) anisotropies to the large-scale structure of the universe [1–3]. However, as observational precision increases, tensions have emerged that suggest the need for physics beyond the standard paradigm. Most notably, recent results from the Dark Energy Spectroscopic Instrument (DESI) 2024, when combined with Supernovae Type Ia (SNIa) and CMB datasets, favor a dynamical dark energy component over a cosmological constant [4, 5]. Specifically, the data prefers an equation of state that crosses the so-called “phantom divide” ($w < -1$) at late times, characterized by the parameter space $w_0 > -1$ and $w_a < 0$ [4, 6–10].

This observational hint poses a significant theoretical challenge. Canonical single-field quintessence models are typically restricted to the region $w \geq -1$ [11, 12], while naive attempts to realize phantom behavior often lead to pathologies such as ghost degrees of freedom or gradient instabilities [13–15]. Consequently, constructing a consistent theoretical framework that explains both the early inflationary epoch and the specific late-time phantom dynamics favored by DESI—without introducing instabilities—remains an open problem [16–18]. However, this issue can be addressed by introducing a non-minimal coupling [19–26]. Although numerous approaches exist to study evolving dark energy—including the Quintom sce-

nario [27–29], $f(R)$ gravitational models [30–32], even using the minimally coupling to investigate the dynamical DE [33] that represents the local effects of DE [34]. We restrict our attention in this paper to the non-minimally coupled dark energy model.

The “Running Curvaton” model [35] was previously proposed as a unified approach to connect early-universe physics with late-time acceleration. In this framework, the curvaton field generates primordial perturbations during inflation and survives to serve as the dark energy candidate today. However, in its original minimally coupled form, the model behaves as a thawing quintessence field, which is theoretically unable to access the phantom regime ($w < -1$) suggested by the new data.

In this paper, we propose an extension of the Running Curvaton model by introducing a non-minimal gravitational coupling of the form $\xi\chi^2R$. We demonstrate that this modification provides the necessary geometric corrections to the effective energy-momentum tensor in the Jordan frame, enabling the equation of state to cross the phantom divide naturally [36–38]. This extension allows the model to populate the $w_0 - w_a$ observational plane favored by DESI 2024, resolving the tension faced by the standard model.

A critical concern when modifying a unified model is whether the new physics spoils successful predictions for the early universe. We address this by deriving a parameter re-tuning scheme. We show that the geometric correction to the effective mass of the curvaton during inflation can be exactly compensated by shifting the coupling parameters. As a result, the standard predictions for the spectral index (n_s) and non-Gaussianity ($f_{NL} \approx 5/4r_{dec}$) are strictly preserved, ensuring consistency with Planck observations [39].

* libichu@mail.ustc.edu.cn

† liuleihua8899@hotmail.com, corresponding author

Furthermore, we rigorously check the stability of the model. By mapping our action to the general Horndeski scalar-tensor theory [40–42], we confirm that the sound speed of scalar perturbations remains positive ($c_s^2 = 1$), guaranteeing that the model is free from gradient instabilities despite the effective phantom equation of state. The local effect of modified gravity is screened due to the high-density environment of the Solar System [43].

The paper is organized as follows: Section II outlines the non-minimally coupled Running Curvaton model. Section III demonstrates the preservation of early-universe perturbation predictions via parameter re-tuning. Section IV analyzes the late-time evolution, deriving the effective equation of state and confronting the model with DESI constraints and stability requirements. Finally, Section V concludes with a discussion of our findings.

II. THE MODEL

We consider the Running Curvaton field χ non-minimally coupled to gravity. The action in the Jordan frame is given by:

$$S = \int d^4x \sqrt{-g} \left[\frac{1}{2} (M_P^2 - \xi \chi^2) R - \frac{1}{2} (\nabla \chi)^2 - V(\chi) \right] + S_m, \quad (1)$$

where M_P denotes the reduced Planck mass, ξ is the coupling constant, and S_m describes the matter sector (comprising the inflaton in the early epoch and standard matter at late times). In this work, we adopt the running curvaton framework proposed in Ref. [44]. Prior to presenting our detailed calculations, we outline the essential features of this model. Recall that in the running curvaton scenario, the curvaton mass evolves due to an explicit coupling between the inflaton and the curvaton, as shown in the potential

$$V(\chi) = \frac{1}{2} \frac{g}{M_P^2} V(\phi) \chi^2 + V_1 (1 - V_0 e^{-\lambda \chi / M_P}), \quad (2)$$

where ϕ denotes the inflaton, while V_1 , V_0 , and λ are parameters constrained by the DESI observations. The first term represents the coupling, which originates from parametric resonance during preheating [45, 46], as discussed in our previous work [44]. This term dominates over the second term, meaning the effective mass is primarily determined by the first part. Consequently, the second part is negligible compared to the first, which we treat as fixed in the following analysis. After the inflaton decays, the first term of the potential (2) vanishes. However, the second term survives, approaching a constant value of the same order as the cosmological constant.

The second part of the curvaton potential (2) is distinct from the original version, $V(\chi) = \frac{1}{2} \frac{g}{M_P^2} V(\phi) \chi^2 + \lambda_0 e^{-\lambda_1 \chi / M_P}$ (where $\lambda_0 \sim V_1$). We modify the potential to the form in Eq. (2) because it provides a better fit

to DESI observations [4, 47], which allows for a dynamic equation of state that better captures the $w_0 - w_a$ evolution suggested by the DESI 2024 data. While the exponential potential in the original model reproduces thawing quintessence (TQ) [48], its CPL parameters (w_0, w_a) are in tension with, or only marginally consistent with, the most recent constraints [49].

The investigations above provide a microscopic origin for dark energy (DE). Drawing on our previous work [44], we summarize the complete picture for DE as follows. During the preheating epoch, the inflaton decays into fundamental particles, such as Higgs bosons and fermions. Simultaneously, a portion of the inflaton energy is transferred to the curvaton via their coupling; this curvaton subsequently generates the curvature perturbations observed in the CMB. Because the curvaton is a light, long-lived field compared to the inflaton, it survives into the late-time universe where the second term of the potential (2) eventually dominates. Due to the non-minimal coupling, the DE equation of state can cross the phantom divide ($w = -1$). In the following sections, we demonstrate that this model is consistent with the original running curvaton framework [44].

III. EARLY-TIME PERTURBATIONS: PRESERVING PREDICTIONS

In the following calculations, we utilize the Friedmann-Lemaître-Robertson-Walker (FLRW) background metric:

$$ds^2 = -dt^2 + a^2(t) \delta_{ij} dx^i dx^j, \quad (3)$$

where $a(t)$ is the scale factor. A primary motivation for the running curvaton model is its ability to generate the observed curvature perturbations. A key concern, however, is whether the introduction of the non-minimal coupling $\xi \chi^2 R$ spoils these successful early-universe predictions. In this section, we demonstrate that the model's consistency is strictly preserved through a straightforward parameter re-tuning. To implement this, we first derive the effective mass of the curvaton.

A. Modified Effective Mass

To derive the effective mass of the curvaton field during inflation, we begin with the Jordan frame action in Eq. (1). The effective curvaton mass can be defined as $m_{\text{eff}}^{\text{cur}} = V''(\bar{\chi})$; alternatively, it can be extracted from the equation of motion (EOM) for the curvaton perturbation. We define the curvaton field as $\chi(x_\mu) = \bar{\chi}(t) + \delta\chi(x_\mu)$, where $\bar{\chi}$ is the homogeneous background and $\delta\chi$ is the perturbation. By substituting this decomposition into the action (1) and expanding to second order in $\delta\chi$, we

obtain the action for the curvaton perturbations:

$$S_{\delta\chi} = \int d^4x \sqrt{-g} \left[-\frac{1}{2} g^{\mu\nu} \partial_\mu \delta\chi \partial_\nu \delta\chi - \frac{1}{2} (V'' + \xi R) \delta\chi^2 \right]. \quad (4)$$

Varying with actionm (4), we could obtain the EOM of curvaton perturbation of curvaton as follows,

$$\frac{1}{\sqrt{-g}} \partial_\mu (\sqrt{-g} g^{\mu\nu} \partial_\nu \delta\chi) - (V''(\bar{\chi}) + \xi R) \delta\chi = 0. \quad (5)$$

Making use of the background metric (3), we could obtain

$$\delta\ddot{\chi} + 3H\delta\dot{\chi} + k^2\delta\chi + (V''(\bar{\chi}) + \xi R) \delta\chi = 0, \quad (6)$$

where we could define effective mass

$$m_{\text{eff}}^2 = m_{\text{orig}}^2 + \xi R \quad (7)$$

where there is geometric correction for the effective mass of curvaton. Based on FLRM metric (3), the Ricci scalar can be easily obtained as

$$R = 6(2H^2 + \dot{H}), \quad (8)$$

where $H = \frac{\dot{a}}{a}$. In light of slow-roll condition, we have $\epsilon = -\frac{\dot{H}}{H^2} \ll 1$. Therefore, the term of $12H^2$ is dominant compared to $6\dot{H}$. The Ricci scalar can be simplified into

$$R \approx 12H^2. \quad (9)$$

Finally, the effective mass of curvaton is explicitly obtained as follows,

$$m_{\text{eff}}^2 = m_{\text{orig}}^2 + 12\xi H^2. \quad (10)$$

From the original [44], the original effective mass in earl universe for curvaton is determined by the coupling part of potential

$$m_{\text{orig}} \approx \frac{g}{M_P^2} m^2 \phi^2 \quad (11)$$

In this calculation, we assume a simple quadratic inflationary potential, $V(\phi) = \frac{1}{2} m_\phi^2 \phi^2$. As indicated by the curvaton potential (2), our framework is versatile enough to incorporate multiple curvaton modes. A distinct advantage of the curvaton mechanism is that it relaxes the constraints on the inflaton potential, removing the necessity for a plateau-like shape.

During the early universe, the energy density is primarily dominated by the inflaton potential. Under the slow-roll approximation, the kinetic term is negligible, and the Hubble parameter is given by:

$$3M_P^2 H^2 \approx \frac{1}{2} m_\phi^2 \phi^2 \implies m_\phi^2 \phi^2 \approx 6M_P^2 H^2. \quad (12)$$

Utilizing this approximation, the original curvaton mass can be expressed in terms of the Hubble parameter as follows:

$$m_{\text{orig}}^2 \approx \frac{g_0}{M_P^2} (6M_P^2 H^2) = 6g_0 H^2, \quad (13)$$

Finally, the effective mass of curvaton in this work can be denoted by

$$m_{\text{eff}}^2 = 6g_0 H^2 + 12\xi H^2 = 6H^2(g_0 + 2\xi), \quad (14)$$

This geometric representation to the mass is the key factor that necessitates the re-tuning of the coupling constant discussed in the following subsection.

B. Re-tuning Scheme

Based on the detailed calculation in Appendix A and based on the effective mass of curvaton (10), we could easily derive the spectral index of curvaton

$$n_\chi - 1 = 4(g_0 + 2\xi) = 4g_0^{\text{obs}}, \quad (15)$$

where we have used the de-Sitter approximation which captures the complete information for curvaton. Compared with the original work [44], where $n_\chi^{\text{orig}} - 1 = \frac{2}{3} \frac{m_{\text{orig}}^2}{H^2}$, it explicitly indicates that the $g_0 + 2\xi$ will re-tune in order to maintain the same value of g_0^{orig} via [44].

C. Non-Gaussianity and Tensor Modes

The local non-Gaussianity parameter f_{NL} in curvaton models is determined by the energy fraction at the time of decay, $r_{\text{dec}} \approx \rho_\chi / \rho_{\text{tot}}$. The energy density of ρ_χ is mainly determined by $\frac{1}{2} m_{\text{eff}}^2 \chi^2$. Through appendix B, the prediction for non-Gaussianity remains:

$$f_{\text{NL}} \approx \frac{5}{4r_{\text{dec}}}, \quad (16)$$

which is consistent with Planck constraints for sufficiently large r_{dec} . In our model with non-minimal coupling $\xi\chi^2 R$, this derivation holds valid due to two reasons:

- **Re-tuning Mechanism:** The parameter re-tuning ($g_0 + 2\xi = g_0^{\text{obs}}$) ensures that the field fluctuations $\delta\chi$ and background value $\bar{\chi}$ during inflation are identical to the standard minimally coupled case.

- **Radiation Domination:** During the decay epoch, the universe is radiation-dominated, implying $R \approx 0$. Thus, the non-minimal coupling term $\xi R \chi^2$ vanishes, and the energy density ρ_χ follows the standard canonical form used above.

Consequently, the prediction $f_{\text{NL}} \approx \frac{5}{4r_{\text{dec}}}$ is preserved.

Finally, regarding tensor perturbations, Appendix C has give the detailed calculation to the tensor mode as shown in Eq. (C7). The non-minimal coupling introduces a correction of order $\mathcal{O}(\chi^2/M_P^2)$ to the tensor power spectrum. Since the curvaton is sub-dominant during inflation, the standard inflationary predictions for

gravitational waves (and the tensor-to-scalar ratio r) are preserved to high accuracy.

In this section, we generally discussed the constraint from the universe. Due to the re-tuning parameter $g_0^{obs} = g_0 + 2\xi$, the Spectral index, Non-Gaussianity and tensor model are all consistent with CMB observations.

IV. LATE-TIME EVOLUTION AND CONSTRAINTS

In this section, we will mainly focus on the evolution of DE originated from curvaton. We need to investigate the stability for our model (1) since many DE models suffer the gradient instabilities [13, 16, 50–52]. For us, we expect our model will not suffer this instability problem. Thus, the stability based on the sound speed is of particular importance.

A. Stability Analysis: Sound Speed

A crucial consistency check for any dark energy model crossing the phantom divide is the stability of scalar perturbations. Specifically, we must ensure that the effective sound speed squared, c_s^2 , remains positive to avoid gradient instabilities.

Our action (Eq. 1) falls within the general Horndeski scalar-tensor theory [40], whose Lagrangian is defined by the functions $G_i(\chi, X)$, where $X \equiv -\frac{1}{2}\nabla_\mu\chi\nabla^\mu\chi$ is the kinetic term. Mapping our non-minimally coupled model to the Horndeski framework, we identify:

$$G_2(\chi, X) = X - V(\chi), \quad (17)$$

$$G_4(\chi, X) = \frac{1}{2}(M_P^2 - \xi\chi^2), \quad (18)$$

$$G_3(\chi, X) = G_5(\chi, X) = 0. \quad (19)$$

Note that our kinetic term is canonical, implying $G_{2,X} = 1$ and $G_{2,XX} = 0$. Furthermore, the non-minimal coupling function G_4 depends solely on the field value χ , so $G_{4,X} = 0$.

The effective sound speed squared for scalar perturbations in Horndeski theory is given by $c_s^2 = \mathcal{F}_S/\mathcal{G}_S$, where \mathcal{F}_S and \mathcal{G}_S are determined by the background evolution. In the absence of derivative couplings (i.e., $G_{4,X} = 0$ and $G_3 = G_5 = 0$), these expressions simplify significantly:

$$\mathcal{F}_S = 2G_{2,X} + \dots = 2, \quad (20)$$

$$\mathcal{G}_S = 2G_{2,X} + 4XG_{2,XX} + \dots = 2. \quad (21)$$

Consequently, the sound speed is:

$$c_s^2 = \frac{\mathcal{F}_S}{\mathcal{G}_S} = 1. \quad (22)$$

This result ($c_s^2 = 1 > 0$) confirms that despite the effective equation of state crossing into the phantom regime ($w_{\text{eff}} < -1$) due to the non-minimal coupling $\xi\chi^2R$, the

scalar field perturbations propagate at the speed of light and are free from gradient instabilities. The phantom behavior in our model is a frame-dependent effect arising from the modified Einstein equations, rather than a pathological kinetic term.

In the following subsection, we will constrain the parameter via the Parameterized Post-Newtonian (PPN) approximation.

B. Screening Mechanism at Solar System Scales

Due to the environmental dependence of the scalar field's dynamics, a feature inherent to non-minimally coupled models, the effective mass squared of the curvaton field is given by Eq. (7):

$$m_{\text{eff}}^2(\chi) = V''(\chi) + \xi R. \quad (23)$$

In the high-density environment of the Solar System, the trace of the Einstein equations dictates that the Ricci scalar tracks the local matter density, $R \approx \rho_{\text{loc}}/M_P^2$. This induces a geometric correction to the mass:

$$m_{\text{loc}}^2 \approx V''(\chi) + \xi \frac{\rho_{\text{loc}}}{M_P^2}. \quad (24)$$

For coupling strengths of order unity ($\xi \sim \mathcal{O}(1)$), the high density of local matter ($\rho_{\text{loc}} \gg \rho_{\text{cosmo}}$) generates a large effective mass for the scalar field locally. This phenomenology is analogous to the Symmetron screening mechanism [53, 54], where the field is pinned to a near-zero value in high-density regions, or the Chameleon mechanism [55], where the field becomes sufficiently heavy to suppress long-range interactions.

Consequently, the interaction range of the fifth force, $\lambda \sim m_{\text{loc}}^{-1}$, becomes significantly smaller than the scale of Solar System experiments ($\lambda \ll \text{AU}$). The scalar interaction is Yukawa-suppressed by a factor of $e^{-m_{\text{loc}}r}$, effectively restoring General Relativity ($\gamma \approx 1$) locally. This screening mechanism allows the model to satisfy local gravity constraints without requiring the cosmological field value χ_0 , which drives the late-time phantom crossing favored by DESI [56], to be negligible.

C. Modified Friedmann Equations

In a flat FLRW universe, the variation of Action (1) yields the modified Friedmann equations (Detailed calculation can be found in Appendix D). Neglecting the inflaton field at late times, we have:

$$3(M_P^2 - \xi\chi^2)H^2 = \rho_m + \frac{1}{2}\dot{\chi}^2 + V(\chi) + 6\xi H\chi\dot{\chi}, \quad (25)$$

and

$$\begin{aligned} -2(M_P^2 - \xi\chi^2)\dot{H} = & \rho_m + \dot{\chi}^2 + 2\xi H\chi\dot{\chi} \\ & - 2\xi(\ddot{\chi}^2 + \chi\ddot{\chi}). \end{aligned} \quad (26)$$

D. Effective Equation of State

To compare with observations, we cast the equations into the standard Einstein form: $3M_P^2 H^2 = \rho_m + \rho_{DE}^{eff}$. The effective dark energy density and pressure in the Jordan frame are defined as:

$$\rho_{DE}^{eff} = \frac{1}{2}\dot{\chi}^2 + V(\chi) + 6\xi H\chi\dot{\chi} + 3\xi\chi^2 H^2, \quad (27)$$

$$\begin{aligned} p_{DE}^{eff} &= \frac{1}{2}\dot{\chi}^2 - V(\chi) - 2\xi(\chi\ddot{\chi} + \dot{\chi}^2) \\ &- 4\xi H\chi\dot{\chi} - \xi\chi^2(2\dot{H} + 3H^2). \end{aligned} \quad (28)$$

The effective equation of state is defined as $w_{eff} = p_{DE}^{eff}/\rho_{DE}^{eff}$. To investigate its evolution numerically, we rewrite the dynamics in terms of redshift z . Using the relation $1+z = 1/a$, we transform the time derivative to $\dot{\chi} = -(1+z)H\chi'$, where the prime denotes differentiation with respect to z . Consequently, we derive the Hubble parameter as a function of z as follows:

$$H^2(z) = \frac{\rho_{m,0}(1+z)^3 + V(\chi)}{3(M_P^2 - \xi\chi^2) - \frac{1}{2}(1+z)^2\chi'^2 + 6\xi(1+z)\chi\chi'}, \quad (29)$$

where $\rho_{m,0}$ is the present value of matter's density. Similarly, we also could derive the derivative of $H(z)$ as follows,

$$H'(z) = -\frac{\dot{H}}{(1+z)H} = \frac{S_1(z) - 2\xi\chi S_2(z)}{(1+z)H\Delta}, \quad (30)$$

where we have defined $S_1(z) = \rho_{m,0}(1+z)^3 + (1-2\xi)(1+z)^2H^2\chi'^2 - 2\xi(1+z)H^2\chi\chi'$, $S_2(z) = 3(1+z)H^2\chi' - V'(\chi) - 12\xi H^2\chi$ and $\Delta = 2(M_P^2 - \xi\chi^2 + 6\xi^2\chi^2)$. Based on eq. (29) and eq. (30), we could numerically simulate the crossing the phantom divide.

E. Crossing the Phantom Divide

While the standard canonical model ($\xi = 0$) is constrained to the quintessence regime ($w \geq -1$), the introduction of non-minimal coupling ($\xi \neq 0$) generates geometric terms proportional to H^2 and \dot{H} that contribute negatively to the effective pressure. Mathematically, achieving a phantom equation of state ($w_{eff} < -1$) necessitates $p_{DE}^{eff} + \rho_{DE}^{eff} < 0$. For our specific action, this condition takes the form:

$$\rho_{DE}^{eff} + p_{DE}^{eff} = \dot{\chi}^2(1-2\xi) + 2\xi(H\chi\dot{\chi} - \chi\ddot{\chi} - \chi^2\dot{H}). \quad (31)$$

By tuning ξ (e.g., small positive values) and given the dynamics of the rolling scalar field, this quantity can become negative, allowing the model to fit the $w(z)$ behavior suggested by DESI 2025 (crossing from $w < -1$ in the past to $w > -1$ today).

To numerically solve the background evolution of the curvaton field, we impose the initial conditions $\dot{\chi}_{ini} = 0$

and set χ_{ini} to a negligible non-zero value. Following Ref. [49], we tune the parameters $\{\xi, \lambda, V_1, V_0\}$ to satisfy the equations of motion, ensuring that the resulting equation of state crosses the phantom divide. Regarding units, we adopt the convention of Ref. [43], where setting $V_1 \approx 3H_0^2\Omega_\varphi$ provides a robust basis for simulating the dark energy evolution with respect to redshift z . Throughout this work, we set $M_P = 1$, and express V_0 in units of $M_P^2 H_0/h$. The parameters λ and χ are dimensionless.

Based on Eqs. (29) and (30), we numerically simulate the redshift dependence of the effective equation of state. As shown in Fig. 1, the non-minimal coupling ξ is the key driver for crossing the phantom divide; specifically, the trajectory approaches the cosmological constant limit ($w \rightarrow -1$) as $\xi \rightarrow 0$. Analyzing Eqs. (27) and (28) reveals that the term $-\xi\chi^2(2\dot{H} + 3H^2)$ contributes a negative pressure correction, suppressing $w(z)$ during late times before it rises again due to field evolution. This allows the non-minimally coupled Running Curvaton to resolve the phantom divide problem without pathological kinetic terms. Furthermore, the parameter freedom in $(\lambda, \chi, V_0, V_1)$ allows the model to be mapped extensively onto the $w_0 - w_a$ observational plane.

F. Constraints from DESI

In this section, we will show our model will be consistent with DESI [4]. In our case, w_0 denotes the present value of $w_{eff}|_{a=1}$. Based on (27) and (28), we could derive

$$w_0 = w_{eff}(a)|_{a=1} = \frac{\frac{1}{2}\dot{\chi}^2 - V(\chi) - 2\xi(\chi\ddot{\chi} + \dot{\chi}^2) - 4\xi H\chi\dot{\chi} - \xi\chi^2(2\dot{H} + 3H^2)}{\frac{1}{2}\dot{\chi}^2 + V(\chi) + 6\xi H\chi\dot{\chi} + 3\xi\chi^2 H^2} \Big|_{z=0}, \quad (32)$$

where $w_{eff}(a) = \frac{p_{DE}^{eff}}{\rho_{DE}^{eff}}$. As for the formula of $w(a)$, it is defined in terms of redshift as follows,

$$w_a = \frac{dw_{eff}}{dz} \Big|_{z=0}. \quad (33)$$

Being armed with these two formulas, we could numerically simulate the w .

Fig. 2, which the shadow part combines all three probes (BAO + CMB + SN Ia), reveals the strongest evidence for dynamical dark energy. Notably, regardless of the specific SN Ia sample used (Pantheon+, Union3, or DESY5), the Λ CDM point ($w_0 = -1, w_a = 0$) lies outside the 95% confidence contours, with the tension level ranging from 2.5σ to 3.9σ . This confirms that the phantom crossing behavior is a robust feature of the combined dataset.

As illustrated in Fig. 2, our theoretical predictions for the Running Curvaton model fall precisely within the 68% confidence region favoured by the DESI Y5 BAO data combined with Supernovae (as shown in Figure 6 of the DESI 2025 VI results [4]). The observational preference for the quadrant $w_0 > -1$ and $w_a < 0$ presents

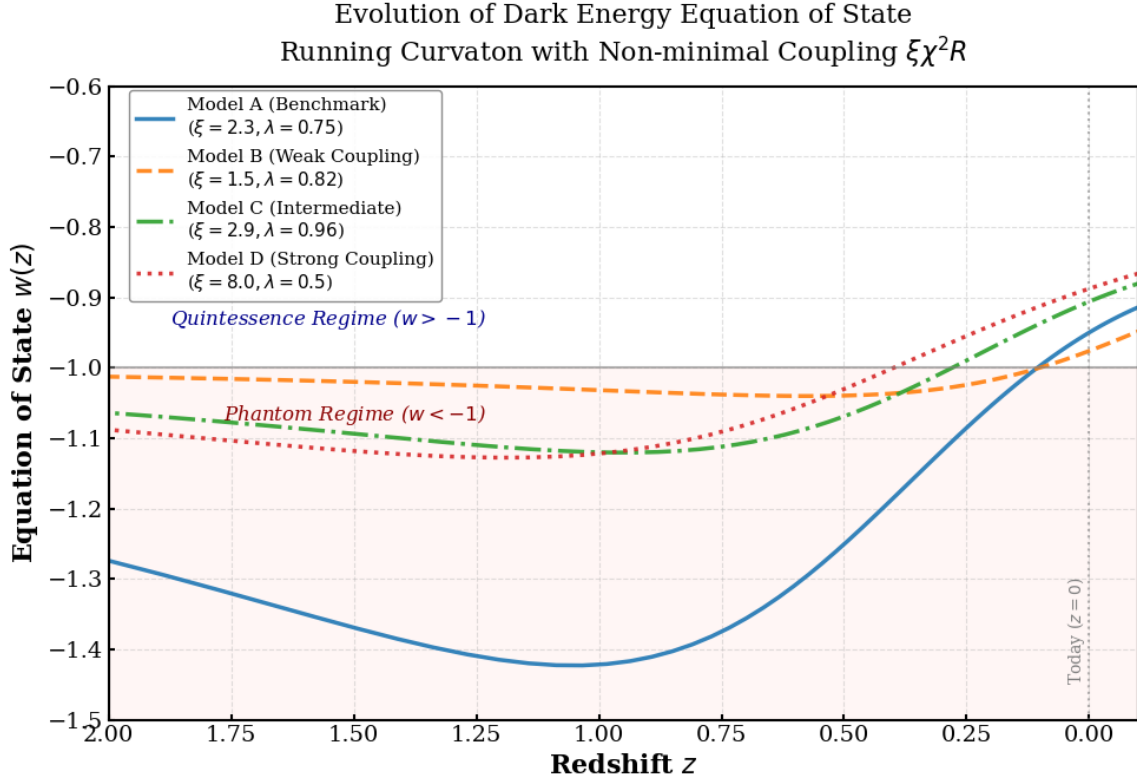


FIG. 1. The evolution for the equation of state $w(z)$. The blue solid line corresponds $(\xi, \lambda, V_0, V_1) = (2.3, 0.75, 0.94, 5.29)$. The green dashed-dotted line is $(\xi, \lambda, V_0, V_1) = (2.1, 1.42, 0.72, 2.24)$. The red dotted line is $(\xi, \lambda, V_0, V_1) = (3.0, 0.5, 0.9, 5.0)$. The orange dashed line is $(\xi, \lambda, V_0, V_1) = (1.5, 0.82, 0.65, 2.67)$. We have set $M_P = 1$ and $\rho_{M,0} = 3M_P^2\Omega_m^0 = 0.93$ with $\Omega_m^0 = 0.31$ and $H_0 = 69 \text{ km s}^{-1} \text{ Mpc}^{-1}$.

a challenge for standard minimally coupled scalar field models, which typically cannot cross the phantom divide ($w = -1$) without theoretical pathologies. Our model successfully populates this specific region through a distinct physical mechanism: the non-minimal coupling $\xi\chi^2R$. Physically, the coupling term induces geometric corrections to the effective energy-momentum tensor. For coupling strengths of order $\xi \sim 2.3$, these corrections generate a sufficient negative contribution to the effective pressure, driving the equation of state $w(z)$ into the phantom regime ($w < -1$) in the past, before evolving back towards quintessence-like behavior ($w > -1$) at present. This "phantom crossing" trajectory is exactly the dynamical feature required to resolve the tension between the DESI BAO measurements and the standard Λ CDM model. Thus, the location of our model in the $w_0 - w_a$ plane is not coincidental but a direct consequence of the geometric interaction governing the field's late-time dynamics.

To constrain the free parameters of the non-minimal coupling model, namely $\theta = \{\xi, \lambda, V_0, V_1\}$, we performed a Monte Carlo parameter scan using the rejection sampling technique. We assumed uniform priors for all parameters within physically motivated ranges: $\xi \in [0, 5]$, $\lambda \in [0, 2]$, $V_0 \in [0.5, 1.5]$, and $V_1 \in [1.0, 6.0]$. For each ran-

domly sampled set of parameters, we numerically solved the background equations of motion (Eq. 32 and Eq. 33) to derive the corresponding dark energy equation-of-state parameters at present day, w_0 , and its evolution, w_a . These theoretical predictions were then mapped onto the observational $w_0 - w_a$ plane. We utilized the 95% confidence level (C.L.) contours obtained from the combination of DESI DR2 BAO, Pantheon+ supernovae, and Planck CMB data as our acceptance criterion. Specifically, we adopted a top-hat likelihood approach: a parameter set was accepted only if its predicted (w_0, w_a) fell within the observational 95% C.L. region; otherwise, it was rejected. Fig. 3 shows the resulting marginalized posterior distributions and 2D confidence regions for the model parameters, derived from 20,000 Monte Carlo trials. Based on the results shown in this figure, the best-fit parameters are $(\xi, \lambda, V_0, V_1) = (2.9, 0.96, 0.76, 3.5)$. We observe that Model B lies almost entirely outside the DESI constraints, as its ξ value is smaller than the minimum threshold of $\xi = 1.6$ shown in Fig. 2. In contrast, Model C aligns well with the best-fit region in Fig. 3. Overall, the results in Fig. 3 demonstrate strong consistency with those presented in Fig. 2.

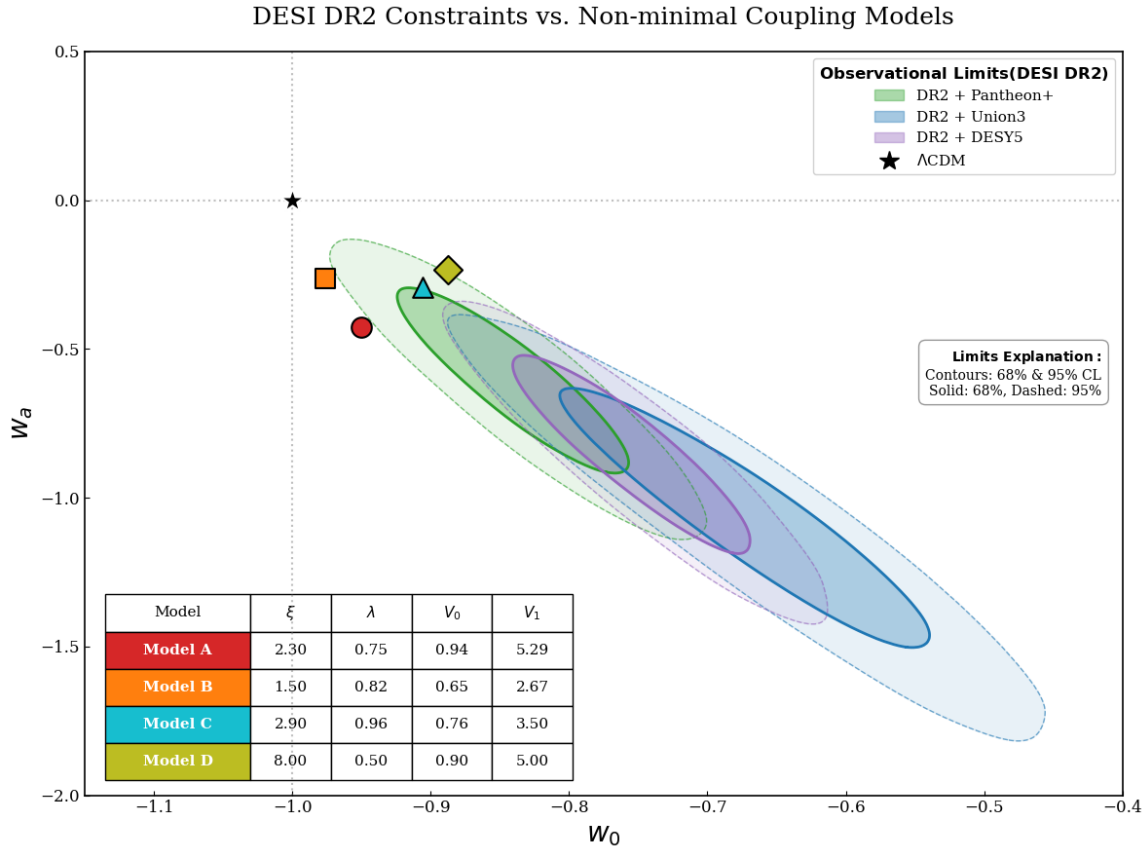


FIG. 2. Observational Constraints vs. Non-minimal Coupling Curvaton. This figure compares the theoretical predictions of our non-minimally coupled Running Curvaton model with the 68% and 95% confidence levels from DESI Y5, Pantheon+, and Union3 datasets. The four distinct models correspond to the four cases in Fig. 1. The black star corresponds to the Λ CDM.

V. DISCUSSION AND CONCLUSION

In this work, we have proposed a unified cosmological framework by extending the Running Curvaton model via a non-minimal gravitational coupling ($\xi\chi^2R$) and a modified self-interaction potential of the form $V(\chi) = V_1(1 - V_0e^{-\lambda\chi/M_P})$. Our investigation demonstrates that this geometric extension successfully reconciles the tension between the standard Λ CDM model and the recent DESI 2024 observations, while strictly preserving the successful predictions of early-universe inflation. The key findings are summarized as follows:

(a). Resolution of the Phantom Divide Crossing

The most significant achievement of this model is its ability to naturally explain the dynamical dark energy evolution favored by DESI 2024 combined with CMB and SNIa data. We showed that the interplay between the non-minimal coupling $\xi\chi^2R$ and the plateau-like potential $V(\chi)$ generates necessary geometric corrections to the effective energy-momentum tensor. This mechanism drives the effective equation of state w_{eff} to cross the phantom divide ($w < -1$) in the past and evolve towards the quintessence regime ($w > -1$) today, precisely populating the observational contour of $w_0 > -1$ and

$w_a < 0$. In light of the most recent DESI 2025 data [4], Fig. 2 demonstrates that our model falls well within the observational confidence contours. Additionally, the corresponding best-fit model parameters are illustrated in Fig. 3.

(b). Preservation of Inflationary Predictions

A critical concern in modified gravity models is the potential disruption of early-universe phenomenology. We addressed this by deriving a robust parameter re-tuning scheme, $g_0^{obs} = g_0 + 2\xi$. We demonstrated that the geometric correction to the curvaton's effective mass during inflation can be exactly compensated by shifting the coupling parameters. Consequently, the standard predictions for the primordial power spectrum (spectral index n_s) and local-type non-Gaussianity ($f_{NL} \approx 5/4r_{dec}$) remain strictly preserved, ensuring the model's consistency with Planck precision data.

(c). Theoretical Stability and Viability

By mapping the action to the general Horndeski scalar-tensor theory, we performed a comprehensive stability analysis. We confirmed that the model is free from pathological ghost and gradient instabilities, maintaining a positive sound speed squared ($c_s^2 = 1$) despite the effective phantom equation of state. Furthermore, our

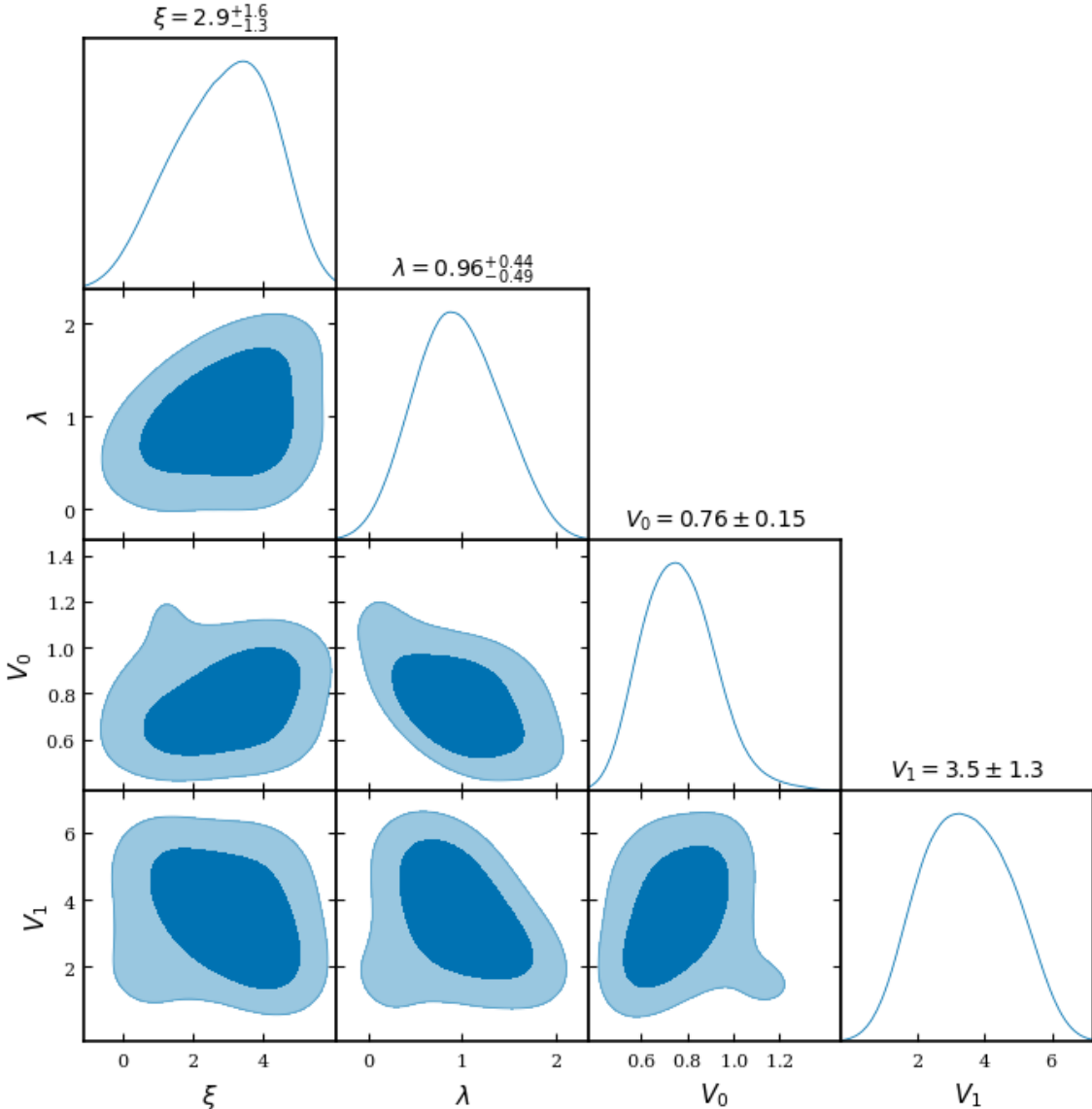


FIG. 3. 68% and 95% C.L. posterior distributions for running curvaton model from the combination of DESI BAO + Pantheon, obtained from sampling uniformly in the parameters via fig. 2.

analysis indicate that the couplings of order $\xi \sim \mathcal{O}(1)$ will not impact the global gravity due to screened mechanism.

In summary, the Non-minimally Coupled Running Curvaton offers a theoretically sound and observationally consistent pathway to unify the physics of the early and late universe. It not only alleviates the current tensions in the dark energy sector but also provides a concrete mechanism for dynamical phantom crossing without violating fundamental stability conditions. Future high-precision surveys, such as Euclid and LSST, will further constrain the derivative of the equation of state, offering a decisive test for the specific $w_0 - w_a$ trajectory predicted by this framework. Furthermore, this work

could be extended into multi-field frameworks [57, 58] and $f(R)$ gravity theories [59–61]. The running curvaton model also provides a mechanism for generating primordial black holes (PBHs) as candidates for dark matter [62]. Additionally, one could investigate the effects of non-minimal coupling on PBH formation.

VI. ACKNOWLEDGMENTS

LH, BC are supported by the National Natural Science Foundation of China (Grant No. 12165009) and the Hunan Natural Science Foundation (Grants No. 2023JJ30487 and No. 2022JJ40340).

[1] N. Aghanim *et al.* (Planck), *Astron. Astrophys.* **641**, A6 (2020), arXiv:1807.06209 [astro-ph.CO].

[2] M. Tegmark *et al.* (SDSS), *Phys. Rev. D* **69**, 103501 (2004), arXiv:astro-ph/0310723.

[3] T. M. C. Abbott *et al.* (DES), *Phys. Rev. D* **105**, 023520 (2022), arXiv:2105.13549 [astro-ph.CO].

[4] G. Gu *et al.* (DESI), *Nature Astron.* **9**, 1879 (2025), [Erratum: *Nature Astron.* 9, 1898 (2025)], arXiv:2504.06118 [astro-ph.CO].

[5] D. Wang, *Phys. Rev. D* **109**, L081303 (2024), arXiv:2404.06310 [astro-ph.CO].

[6] D. Rubin *et al.* (Supernova Union), (2023), arXiv:2311.12098 [astro-ph.CO].

[7] D. Brout *et al.* (Pantheon+), *Astrophys. J.* **938**, 110 (2022), arXiv:2202.04077 [astro-ph.CO].

[8] T. M. C. Abbott *et al.* (DES), (2024), arXiv:2401.02929 [astro-ph.CO].

[9] E. O. Colgáin *et al.*, (2024), arXiv:2404.08633 [astro-ph.CO].

[10] J. Pan and G. Ye, (2025), arXiv:2503.19898 [astro-ph.CO].

[11] R. R. Caldwell, R. Dave, and P. J. Steinhardt, *Phys. Rev. Lett.* **80**, 1582 (1998), arXiv:astro-ph/9708069.

[12] I. Zlatev, L.-M. Wang, and P. J. Steinhardt, *Phys. Rev. Lett.* **82**, 896 (1999), arXiv:astro-ph/9807002.

[13] A. Vikman, *Phys. Rev. D* **71**, 023515 (2005), arXiv:astro-ph/0407107.

[14] W. Hu, *Phys. Rev. D* **71**, 047301 (2005), arXiv:astro-ph/0410680.

[15] R. R. Caldwell, M. Kamionkowski, and N. N. Weinberg, *Phys. Rev. Lett.* **91**, 071301 (2003), arXiv:astro-ph/0302506.

[16] P. Creminelli, G. D'Amico, J. Norena, and F. Vernizzi, *JCAP* **02**, 018 (2009), arXiv:0811.0827 [astro-ph].

[17] B. Feng, X.-G. Wang, and X.-M. Zhang, *Phys. Lett. B* **607**, 35 (2005), arXiv:astro-ph/0404224.

[18] S. Nojiri, S. D. Odintsov, and S. Tsujikawa, *Phys. Rev. D* **71**, 063004 (2005), arXiv:hep-th/0501025.

[19] Z. Yao, G. Ye, and A. Silvestri, *JCAP* **10**, 078 (2025), arXiv:2508.01378 [gr-qc].

[20] W. J. Wolf, P. G. Ferreira, and C. García-García, *Phys. Rev. D* **113**, 023551 (2026), arXiv:2509.17586 [astro-ph.CO].

[21] Y. Tiwari, U. Upadhyay, and R. K. Jain, *Phys. Rev. D* **111**, 043530 (2025), arXiv:2412.00931 [astro-ph.CO].

[22] S. Sánchez López, A. Karam, and D. K. Hazra, (2025), arXiv:2510.14941 [astro-ph.CO].

[23] J.-Q. Wang, R.-G. Cai, Z.-K. Guo, and S.-J. Wang, (2025), arXiv:2508.01759 [astro-ph.CO].

[24] A. Tita, B. Gumjudpai, and P. Srisawad, *Gen. Rel. Grav.* **57**, 106 (2025), arXiv:2507.05273 [gr-qc].

[25] W. J. Wolf, C. García-García, T. Anton, and P. G. Ferreira, *Phys. Rev. Lett.* **135**, 081001 (2025), arXiv:2504.07679 [astro-ph.CO].

[26] H. Adam, M. P. Hertzberg, D. Jiménez-Aguilar, and I. Khan, (2025), arXiv:2509.13302 [astro-ph.CO].

[27] Y. Cai, X. Ren, T. Qiu, M. Li, and X. Zhang, (2025), arXiv:2505.24732 [astro-ph.CO].

[28] Y. Yang, Q. Wang, X. Ren, E. N. Saridakis, and Y.-F. Cai, *Astrophys. J.* **988**, 123 (2025), arXiv:2504.06784 [astro-ph.CO].

[29] Y. Yang, X. Ren, Q. Wang, Z. Lu, D. Zhang, Y.-F. Cai, and E. N. Saridakis, *Sci. Bull.* **69**, 2698 (2024), arXiv:2404.19437 [astro-ph.CO].

[30] S. Nojiri, S. D. Odintsov, and V. K. Oikonomou, (2025), arXiv:2512.06279 [gr-qc].

[31] S. Nojiri, S. D. Odintsov, and V. K. Oikonomou, *Phys. Rev. D* **112**, 104035 (2025), arXiv:2506.21010 [gr-qc].

[32] S. D. Odintsov and V. K. Oikonomou, (2026), arXiv:2601.21364 [gr-qc].

[33] I. D. Gialamas, G. Hützi, M. Raidal, J. Urrutia, M. Vasar, and H. Veermäe, *Phys. Rev. D* **112**, 063551 (2025), arXiv:2506.21542 [astro-ph.CO].

[34] I. D. Gialamas, G. Hützi, K. Kannike, A. Racioppi, M. Raidal, M. Vasar, and H. Veermäe, *Phys. Rev. D* **111**, 043540 (2025), arXiv:2406.07533 [astro-ph.CO].

[35] L.-H. Liu and W.-L. Xu, *Chin. Phys. C* **44**, 085103 (2020), arXiv:2001.02929 [astro-ph.CO].

[36] V. Faraoni, *Phys. Rev. D* **62**, 023504 (2000), arXiv:gr-qc/0002091.

[37] E. Elizalde, S. Nojiri, and S. D. Odintsov, *Phys. Rev. D* **70**, 043539 (2004), arXiv:hep-th/0405034.

[38] R. Gannouji, D. Polarski, A. Ranquet, and A. A. Starobinsky, *JCAP* **09**, 016 (2006), arXiv:astro-ph/0606287.

[39] Y. Akrami *et al.* (Planck), *Astron. Astrophys.* **641**, A10 (2020), arXiv:1807.06211 [astro-ph.CO].

[40] G. W. Horndeski, *Int. J. Theor. Phys.* **10**, 363 (1974).

[41] C. Deffayet, X. Gao, D. A. Steer, and G. Zahariade, *Phys. Rev. D* **84**, 064039 (2011), arXiv:1103.3260 [hep-th].

[42] T. Kobayashi, M. Yamaguchi, and J. Yokoyama, *Prog. Theor. Phys.* **126**, 511 (2011), arXiv:1105.5723 [hep-th].

[43] G. Ye, M. Martinelli, B. Hu, and A. Silvestri, *Phys. Rev. Lett.* **134**, 181002 (2025), arXiv:2407.15832 [astro-ph.CO].

[44] L.-H. Liu and W.-L. Xu, *Chin. Phys. C* **44**, 085103 (2020).

[45] L. Kofman, A. D. Linde, and A. A. Starobinsky, *Phys. Rev. Lett.* **73**, 3195 (1994), arXiv:hep-th/9405187 [hep-th].

[46] L. Kofman, A. D. Linde, and A. A. Starobinsky, *Phys. Rev. D* **56**, 3258 (1997), arXiv:hep-ph/9704452 [hep-ph].

[47] M. Abdul Karim *et al.* (DESI), *Phys. Rev. D* **112**, 083515 (2025), arXiv:2503.14738 [astro-ph.CO].

[48] W. J. Wolf and P. G. Ferreira, *Phys. Rev. D* **108**, 103519 (2023), arXiv:2310.07482 [astro-ph.CO].

[49] W. J. Wolf, C. García-García, D. J. Bartlett, and P. G. Ferreira, *Phys. Rev. D* **110**, 083528 (2024), arXiv:2408.17318 [astro-ph.CO].

[50] G. Gubitosi, F. Piazza, and F. Vernizzi, *JCAP* **02**, 032 (2013), arXiv:1210.0201 [hep-th].

[51] W. J. Wolf and M. Lagos, *Phys. Rev. D* **100**, 084035 (2019), arXiv:1908.03212 [gr-qc].

[52] P. Creminelli, G. Tambalo, F. Vernizzi, and V. Yingcharoenrat, *JCAP* **05**, 002 (2020), arXiv:1910.14035 [gr-qc].

[53] K. Hinterbichler and J. Khoury, *Phys. Rev. Lett.* **104**, 231301 (2010), arXiv:1001.4525 [hep-th].

[54] J. Khoury, (2010), 10.48550/arXiv.1011.5909, arXiv:1011.5909 [astro-ph.CO].

- [55] J. Khoury and A. Weltman, Phys. Rev. Lett. **93**, 171104 (2004), arXiv:astro-ph/0309300.
- [56] G. Ye, M. Martinelli, B. Hu, and A. Silvestri, (2024), arXiv:2407.15832 [astro-ph.CO].
- [57] L.-H. Liu and T. Prokopec, JCAP **06**, 033 (2021), arXiv:2005.11069 [astro-ph.CO].
- [58] X.-z. Zhang, L.-h. Liu, and T. Qiu, Phys. Rev. D **107**, 043510 (2023), arXiv:2207.07873 [hep-th].
- [59] L.-H. Liu, (2018), 10.1007/s10773-018-3809-0, arXiv:1807.00666 [gr-qc].
- [60] L.-H. Liu, T. Prokopec, and A. A. Starobinsky, Phys. Rev. D **98**, 043505 (2018), arXiv:1806.05407 [gr-qc].
- [61] L.-H. Liu, B. Liang, Y.-C. Zhou, X.-D. Liu, W.-L. Xu, and A.-C. Li, Phys. Rev. D **103**, 063515 (2021), arXiv:2007.08278 [astro-ph.CO].
- [62] L.-H. Liu, Chin. Phys. C **47**, 015105 (2023), arXiv:2107.07310 [astro-ph.CO].

Appendix A: Derivation of the Spectral Index with Non-minimal Coupling

In this appendix, we provide a detailed derivation of the spectral index n_χ for the curvaton field non-minimally coupled to gravity. We show that the geometric correction to the effective mass leads directly to the modified spectral tilt used in our re-tuning mechanism.

1. Perturbation Equation of Motion

Starting from the action in the Jordan frame as given in (1), we consider the linear perturbations of the curvaton field $\chi(t, \mathbf{x}) = \bar{\chi}(t) + \delta\chi(t, \mathbf{x})$. In the flat FLRW background $ds^2 = -dt^2 + a^2(t)d\mathbf{x}^2$, the equation of motion for the Fourier mode $\delta\chi_k$ is given by:

$$\ddot{\delta\chi}_k + 3H\dot{\delta\chi}_k + \left(\frac{k^2}{a^2} + m_{\text{eff}}^2\right)\delta\chi_k = 0, \quad (\text{A1})$$

where the effective mass squared m_{eff}^2 includes the geometric contribution from the non-minimal coupling:

$$m_{\text{eff}}^2 \equiv V''(\bar{\chi}) + \xi R. \quad (\text{A2})$$

During slow-roll inflation, the Ricci scalar is dominated by the Hubble expansion, $R = 6(2H^2 + \dot{H}) \approx 12H^2$. Thus, the effective mass becomes:

$$m_{\text{eff}}^2 \approx V''(\bar{\chi}) + 12\xi H^2. \quad (\text{A3})$$

2. Reduction to Bessel Equation

To solve Eq. (A1), we switch to conformal time $\tau = \int dt/a(t)$ and define the canonical variable $u_k(\tau) = a(\tau)\delta\chi_k(\tau)$. The evolution equation transforms into:

$$u_k'' + \left(k^2 - \frac{a''}{a} + a^2 m_{\text{eff}}^2\right)u_k = 0. \quad (\text{A4})$$

In the de Sitter limit ($a \approx -1/H\tau$), the effective potential term becomes $(a''/a - a^2 m_{\text{eff}}^2) \approx \frac{1}{\tau^2}(2 - m_{\text{eff}}^2/H^2)$. Consequently, the mode equation takes the form of a Bessel equation:

$$u_k'' + \left(k^2 - \frac{\nu^2 - 1/4}{\tau^2}\right)u_k = 0, \quad (\text{A5})$$

where the order ν is defined by:

$$\nu = \sqrt{\frac{9}{4} - \frac{m_{\text{eff}}^2}{H^2}}. \quad (\text{A6})$$

3. Power Spectrum and Spectral Index

The solution matching the Bunch-Davies vacuum at early times ($|k\tau| \gg 1$) is given by the Hankel function of the first kind:

$$u_k(\tau) = \frac{\sqrt{\pi}}{2}\sqrt{-\tau}H_\nu^{(1)}(-k\tau). \quad (\text{A7})$$

On super-horizon scales ($|k\tau| \ll 1$), the asymptotic behavior of the Hankel function yields the power spectrum $\mathcal{P}_{\delta\chi} \equiv \frac{k^3}{2\pi^2}|\delta\chi_k|^2$:

$$\mathcal{P}_{\delta\chi}(k) \propto k^{3-2\nu}. \quad (\text{A8})$$

The spectral index is defined as $n_\chi - 1 \equiv d\ln \mathcal{P}_{\delta\chi}/d\ln k = 3 - 2\nu$. For a light field ($m_{\text{eff}}^2 \ll H^2$), we expand ν to first order:

$$\nu \approx \frac{3}{2}\left(1 - \frac{2}{3}\frac{m_{\text{eff}}^2}{3H^2}\right) = \frac{3}{2} - \frac{m_{\text{eff}}^2}{3H^2}. \quad (\text{A9})$$

Substituting this back into the expression for n_χ , we arrive at the standard result modified by the effective mass:

$$n_\chi - 1 \approx \frac{2}{3}\frac{m_{\text{eff}}^2}{H^2}. \quad (\text{A10})$$

Substituting the explicit form of the mass $m_{\text{eff}}^2 = m_{\text{orig}}^2 + 12\xi H^2$, we obtain:

$$n_\chi - 1 \approx \frac{2}{3}\frac{m_{\text{orig}}^2}{H^2} + 8\xi. \quad (\text{A11})$$

This linear dependence on ξ necessitates the parameter re-tuning strategy ($g_0 \rightarrow g_0 - 2\xi$) discussed in Section III to preserve consistency with Planck observations.

Appendix B: Detailed Calculation of Non-Gaussianity f_{NL}

In this appendix, we will derive the specific form of the non-linearity parameter f_{NL} .

1. Curvature Perturbation Expansion

The curvature perturbation ζ on uniform density hypersurfaces is related to the energy density fluctuation $\delta\rho$ by:

$$\zeta = -H \frac{\delta\rho}{\dot{\rho}} = \frac{1}{3} \frac{\delta\rho}{\rho}, \quad (\text{B1})$$

assuming the universe is dominated by a fluid with equation of state $w \approx 0$ (oscillating curvaton) or considering the decay into radiation.

For the curvaton field χ , the energy density is given by $\rho_\chi \approx m_{\text{eff}}^2 \chi^2/2$. The density perturbation, expanded to second order in the field fluctuation $\delta\chi$, is:

$$\begin{aligned} \rho_\chi(\bar{\chi} + \delta\chi) &= \frac{1}{2} m_{\text{eff}}^2 (\bar{\chi} + \delta\chi)^2 \\ &= \frac{1}{2} m_{\text{eff}}^2 \bar{\chi}^2 \left(1 + 2 \frac{\delta\chi}{\bar{\chi}} + \left(\frac{\delta\chi}{\bar{\chi}} \right)^2 \right). \end{aligned} \quad (\text{B2})$$

Thus, the density contrast is:

$$\frac{\delta\rho_\chi}{\rho_\chi} = 2 \frac{\delta\chi}{\bar{\chi}} + \left(\frac{\delta\chi}{\bar{\chi}} \right)^2. \quad (\text{B3})$$

2. Transfer to Adiabatic Perturbation

Using the sudden decay approximation, the total curvature perturbation ζ is a weighted sum of the inflaton and curvaton perturbations. Assuming the inflaton contribution is negligible, ζ is given by:

$$\zeta \approx r_{\text{dec}} \zeta_\chi = \frac{r_{\text{dec}}}{3} \frac{\delta\rho_\chi}{\rho_\chi}, \quad (\text{B4})$$

where $r_{\text{dec}} \equiv \frac{3\rho_\chi}{3\rho_\chi + 4\rho_\gamma} \Big|_{\text{decay}} \approx \frac{\rho_\chi}{\rho_{\text{tot}}}$ is the energy fraction of the curvaton at the time of decay (in the limit $r_{\text{dec}} \ll 1$).

Substituting the expansion of $\delta\rho_\chi/\rho_\chi$:

$$\zeta = \frac{r_{\text{dec}}}{3} \left[2 \frac{\delta\chi}{\bar{\chi}} + \left(\frac{\delta\chi}{\bar{\chi}} \right)^2 \right]. \quad (\text{B5})$$

3. Identifying f_{NL}

We decompose ζ into a Gaussian part ζ_g (linear term) and a non-Gaussian correction. From Eq. (B5), the linear Gaussian part is:

$$\zeta_g = \frac{2r_{\text{dec}}}{3} \frac{\delta\chi}{\bar{\chi}}. \quad (\text{B6})$$

We can express the quadratic term $(\delta\chi/\bar{\chi})^2$ in terms of ζ_g :

$$\left(\frac{\delta\chi}{\bar{\chi}} \right)^2 = \left(\frac{3}{2r_{\text{dec}}} \zeta_g \right)^2 = \frac{9}{4r_{\text{dec}}^2} \zeta_g^2. \quad (\text{B7})$$

Now, substituting this back into Eq. (B5):

$$\zeta = \zeta_g + \frac{r_{\text{dec}}}{3} \left(\frac{9}{4r_{\text{dec}}^2} \zeta_g^2 \right) = \zeta_g + \frac{3}{4r_{\text{dec}}} \zeta_g^2. \quad (\text{B8})$$

The standard definition of the local non-linearity parameter f_{NL} is given by the expansion:

$$\zeta = \zeta_g + \frac{3}{5} f_{NL} \zeta_g^2. \quad (\text{B9})$$

Comparing the coefficients of the ζ_g^2 term:

$$\frac{3}{5} f_{NL} = \frac{3}{4r_{\text{dec}}} \implies f_{NL} = \frac{5}{4r_{\text{dec}}}. \quad (\text{B10})$$

Appendix C: Tensor Perturbations with Non-minimal Coupling

In this appendix, we verify the stability of the tensor perturbations and estimate the corrections to the primordial gravitational waves induced by the non-minimal coupling term $\xi\chi^2 R$.

1. Second-Order Action for Tensor Modes

We consider the tensor perturbations to the metric in the Jordan frame, defined as $g_{ij} = a^2(\tau)(\delta_{ij} + h_{ij})$, where h_{ij} satisfies the transverse-traceless conditions ($\partial^i h_{ij} = 0$, $h_i^i = 0$). The second-order action for tensor modes arising from the gravitational sector of Eq. (1) is given by:

$$S_h = \frac{1}{8} \int d\tau d^3x a^2 \Omega(\chi) [(h'_{ij})^2 - (\nabla h_{ij})^2], \quad (\text{C1})$$

where primes denote derivatives with respect to conformal time τ . The non-minimal coupling modifies the effective Planck mass squared:

$$M_{\text{eff}}^2(\chi) \equiv \Omega(\chi) = M_P^2 - \xi\chi^2. \quad (\text{C2})$$

2. Evolution Equation

To diagonalize the kinetic term, we define the canonical variable $v_k(\tau) = z_T h_k(\tau)$ for each polarization mode, with the pump field defined as:

$$z_T(\tau) = \frac{a(\tau)}{2} \sqrt{\Omega(\chi)}. \quad (\text{C3})$$

The equation of motion (Mukhanov-Sasaki equation) for the mode function v_k in Fourier space is:

$$v_k'' + \left(k^2 - \frac{z_T''}{z_T} \right) v_k = 0. \quad (\text{C4})$$

During slow-roll inflation, the curvaton field χ is effectively frozen (or evolving very slowly compared to the expansion), so $\Omega(\chi) \approx \text{const}$. In the de Sitter limit where $a(\tau) \approx -1/(H\tau)$, the effective mass term simplifies to:

$$\frac{z_T''}{z_T} \approx \frac{a''}{a} \approx \frac{2}{\tau^2}. \quad (\text{C5})$$

This indicates that the evolution of tensor modes remains effectively the same as in General Relativity, up to a rescaling of the normalization factor z_T .

3. Primordial Power Spectrum

Solving the mode equation with Bunch-Davies vacuum initial conditions leads to the primordial tensor power spectrum on super-horizon scales:

$$\mathcal{P}_T(k) = \frac{2H^2}{\pi^2 M_{\text{eff}}^2} = \frac{2H^2}{\pi^2 (M_P^2 - \xi \chi_*^2)}, \quad (\text{C6})$$

where quantities are evaluated at the horizon exit. We can express this relative to the standard GR prediction $\mathcal{P}_{T,GR} \approx \frac{2H^2}{\pi^2 M_P^2}$:

$$\mathcal{P}_T(k) = \mathcal{P}_{T,GR} \left[1 - \xi \left(\frac{\chi_*}{M_P} \right)^2 \right]^{-1} \approx \mathcal{P}_{T,GR} \left[1 + \xi \frac{\chi_*^2}{M_P^2} \right]. \quad (\text{C7})$$

4. Consistency Check: Sub-dominance Condition

The validity of our model relies on the assumption that the curvaton χ is a spectator field during inflation, meaning its energy density is negligible compared to the inflaton, and its field value is sub-Planckian:

$$\chi_* \ll M_P \implies \frac{\chi_*^2}{M_P^2} \ll 1. \quad (\text{C8})$$

Assuming the field does not traverse trans-Planckian distances from inflation to today, the correction term $\xi(\chi/M_P)^2$ remains negligible throughout cosmic history.

Appendix D: Appendix: Derivation of the Effective Equation of State

We consider the Running Curvaton model extended with a non-minimal gravitational coupling in the Jordan Frame. The action is given by (1), where the non-minimal coupling function is defined as:

$$\Omega(\chi) = M_P^2 - \xi \chi^2. \quad (\text{D1})$$

Then, we will vary with respect to this action for the gravitational sector, matter sector and dark energy sector, respectively. First, let us vary with the gravitational sector $\delta S_g = \frac{1}{2} \int d^4x \delta(\sqrt{-g}\Omega(\chi)R)$. Essentially,

we need to deal with

$$\begin{aligned} \delta(\sqrt{-g}\Omega R) &= (\delta\sqrt{-g})\Omega R + \sqrt{-g}\Omega(\delta R) \\ &= -\frac{1}{2}\sqrt{-g}g_{\mu\nu}\Omega R\delta g^{\mu\nu} + \sqrt{-g}\Omega(R_{\mu\nu}\delta g^{\mu\nu} + g_{\mu\nu}\square\delta g^{\mu\nu} \\ &\quad - \nabla_\mu\nabla_\nu\delta g^{\mu\nu}). \end{aligned} \quad (\text{D2})$$

Since $\Omega(\chi)$ is not a constant, the total divergence term in δR cannot be discarded. We perform integration by parts to shift the derivatives onto Ω :

$$\begin{aligned} \int d^4x \sqrt{-g}\Omega(g_{\mu\nu}\square - \nabla_\mu\nabla_\nu)\delta g^{\mu\nu} &= \\ \int d^4x \sqrt{-g}(g_{\mu\nu}\square\Omega - \nabla_\mu\nabla_\nu\Omega)\delta g^{\mu\nu}. \end{aligned} \quad (\text{D3})$$

Combining these terms, the variation of the gravitational sector is:

$$\frac{\delta S_g}{\delta g^{\mu\nu}} = \sqrt{-g} \left[\frac{1}{2}\Omega(R_{\mu\nu} - \frac{1}{2}g_{\mu\nu}R) + \frac{1}{2}(g_{\mu\nu}\square\Omega - \nabla_\mu\nabla_\nu\Omega) \right]. \quad (\text{D4})$$

Nextly, we will vary with respect to the curvaton part. This is the standard result for a canonical scalar field:

$$\begin{aligned} \frac{\delta S_\chi}{\delta g^{\mu\nu}} &= \frac{\delta}{\delta g^{\mu\nu}} \int d^4x \sqrt{-g} \left[\frac{1}{2}\Omega R - \frac{1}{2}g^{\mu\nu}\nabla_\mu\chi\nabla_\nu\chi - V \right] \\ &= \left(-\frac{1}{2}\sqrt{-g}g_{\mu\nu} \right) \left(-\frac{1}{2}\nabla_\rho\chi\nabla^\rho\chi - V \right) + \sqrt{-g} \left(-\frac{1}{2}\nabla_\mu\chi\nabla_\nu\chi \right) \\ &= \sqrt{-g} \left(-\frac{1}{2}\nabla_\mu\chi\nabla_\nu\chi + \frac{1}{4}g_{\mu\nu}(\nabla\chi)^2 + \frac{1}{2}g_{\mu\nu}V(\chi) \right). \end{aligned} \quad (\text{D5})$$

Combined with the above results, we could derive the modified Einstein equation under the Jordan frame as follows,

$$\Omega(\chi)G_{\mu\nu} = T_{\mu\nu}^{(m)} + T_{\mu\nu}^{(\chi)} + \nabla_\mu\nabla_\nu\Omega(\chi) - g_{\mu\nu}\square\Omega(\chi), \quad (\text{D6})$$

where $T_{\mu\nu}^{(\chi)} = \nabla_\mu\chi\nabla_\nu\chi - g_{\mu\nu}[\frac{1}{2}(\nabla\chi)^2 + V(\chi)]$ is the energy-momentum tensor of the scalar field.

In this work, we will adopt the conformal flat FRW metric (3). In light of this background metric, the non-vanishing elements for the modified Einstein equations are summarized as

$$G_{00} = 3H^2, G_{ij} = -a^2\eta_{ij}(-3H^2 - 2\dot{H}), \quad (\text{D7})$$

Keeping in mind that χ only depends on the time. Thus, we have $\square\Omega = g^{\mu\nu}\nabla_\mu\nabla_\nu\Omega = -\ddot{\Omega} - 3H\dot{\Omega}$ and $\nabla_0\nabla_0\Omega = \ddot{\Omega}$, $\nabla_i\nabla_j\Omega = -\Gamma_{ij}^0\dot{\Omega} = -a^2H\delta_{ij}\dot{\Omega}$.

Taking these calculations into account, we first could derive the 00 component of the modified Einstein equation (D6) as follows,

$$3(M_P^2 - \xi\chi^2)H^2 = \rho_m + \frac{1}{2}\dot{\chi}^2 + V(\chi) + 6\xi H\chi\dot{\chi}. \quad (\text{D8})$$

Similarly, we could derive the ij component for Einstein equation as

$$\Omega(\chi) \left(-2\dot{H} - 3H^2 \right) = p_m - \left(-\frac{1}{2}\dot{\chi}^2 + V(\chi) \right) - (2\xi(\dot{\chi}^2 + \chi\ddot{\chi}) + 4\xi H\chi\dot{\chi}) \quad (\text{D9})$$

During these calculations, we have utilized

$$\dot{\Omega} = -2\xi\chi\dot{\chi}, \quad (\text{D10})$$

$$\ddot{\Omega} = -2\xi(\dot{\chi}^2 + \chi\ddot{\chi}). \quad (\text{D11})$$

We recast the modified Friedmann equations into the standard Einsteinian form to define effective dark energy quantities:

$$3M_P^2 H^2 = \rho_m + \rho_{DE}^{eff}, \quad (\text{D12})$$

$$-2M_P^2 \dot{H} = (\rho_m + p_m) + (\rho_{DE}^{eff} + p_{DE}^{eff}). \quad (\text{D13})$$

According to these two definitions, we could easily obtain the effective energy density (27) and pressure (28) for DE induced by the curvaton.